MnZn Ferrite Material
(EPCOS N87)
datasheet

Ferrite (N87) core materials are an oxide made from Fe (iron), Mn (manganese), and Zn (zinc), which are commonly referred to as manganese zinc ferrites. They exhibit good magnetic properties (high permeability and saturation induction) below the Curie temperature and have a rather high electrical resistivity. These materials can be used up to very high frequencies (up to 3 MHz) without laminating, as is the normal requirement for magnetic materials to reduce eddy current losses. Because of their comparatively low losses at high frequencies, they form an essential part of inductors and transformers used in today's main application areas of telecommunications, power conversion, and interference suppression. They are produced in a variety of shapes, including toroids, E-cores, U-cores, I-cores, and pot cores.

Fig. 1: Core under test (Ferrite core)

MnZn Ferrite (N87) core

Date: September 2018
Revision 0.1

Dimensions

Table 1: Core dimensions

Description	Symbol	Finished dimension (mm)
Width of core	A	141
Height of core	B	157
Depth of core (or cast width)	D	30
Thickness or build	E	41
Width of core window	F	50
Height of core window	G	67
Gap width	H	Minimum (cut surface to cut surface)

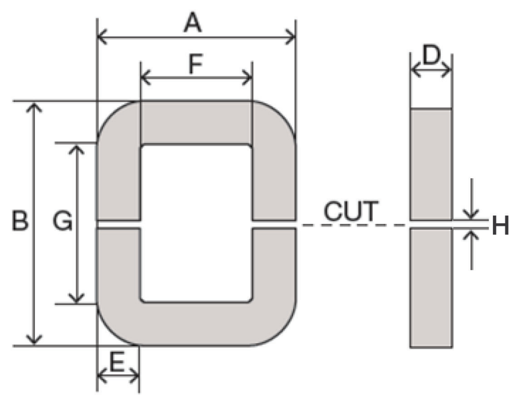

Fig. 2: Illustration of core dimensions

Acknowledgement

This technical effort was performed in support of the National Energy Technology Laboratory's ongoing research in DOE's The Office of Electricity's (OE) Transformer Resilience and Advanced Components (TRAC) program under the RES contract DE-FE0004000.

NATIONAL ENERGY TECHNOLOGY LABORATORY

Magnetic Characteristics

Table 2: Core physical characteristics

Description	Symbol	Typical value	Unit
Effective area	A_e	1,350	mm[2]
Mean magnetic path length[1]	L_m	377	mm
Outer diameter		170.6	mm
Inner diameter		80.6	mm
Weight	*Weight*	2.5	kg
Grade		Ferrite N87	
Supplier		TDK/Epcos	

Measurement Setup

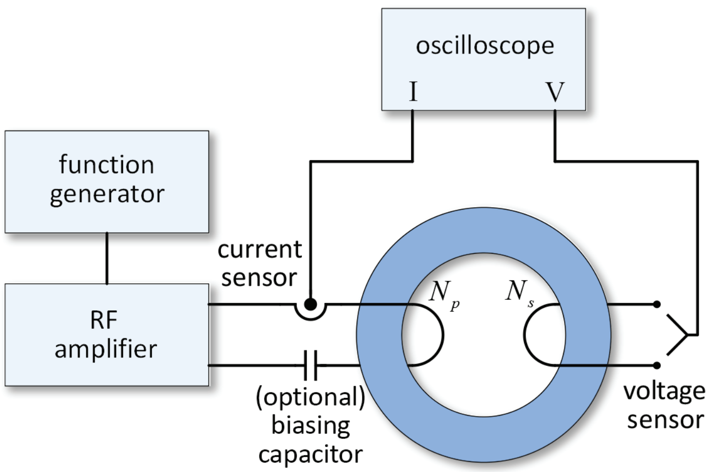

(a)

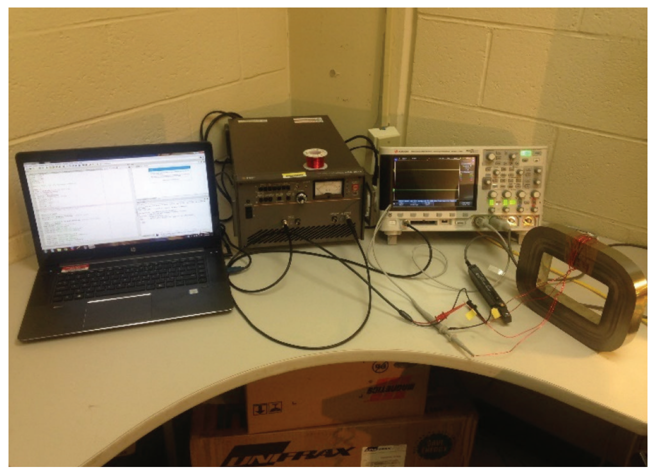
(b)

Fig. 3: Arbitrary waveform core loss test system (CLTS) (a) conceptual setup (b) actual setup

The *BH* curves, core losses, and permeability of the core under test (CUT) are measured with an arbitrary waveform core loss test system (CLTS), which is shown in Fig. 3. Arbitrary small signal sinusoidal waveforms are generated from a function generator, and the small signals are amplified via an amplifier.

Two windings are placed around the core under test. The amplifier excites the primary winding, and the current of the primary winding is measured, in which the current information is converted to the magnetic field strengths *H* as

$$H(t) = \frac{N_p \cdot i(t)}{l_m}, \tag{1}$$

where N_p is the number of turns in the primary winding. A dc-biasing capacitor is inserted in series with the primary winding to provide zero average voltage applied to the primary winding.

---

[1] Mean magnetic path length is computed using the following equation. OD and ID are outer and inner diameters, respectively. $L_m = \dfrac{\pi(\mathrm{OD} - \mathrm{ID})}{\ln\left(\dfrac{\mathrm{OD}}{\mathrm{ID}}\right)}$

The secondary winding is open, and the voltage across the secondary winding is measured, in which the voltage information is integrated to derive the flux density B as

$$B(t) = \frac{1}{N_s \cdot A_e} \int_0^T v(\tau)\, d\tau \quad , \tag{2}$$

where N_s is the number of turns in the secondary winding, and T is the period of the excitation waveform.

Fig. 4 illustrates three different excitation voltage waveforms and corresponding flux density waveforms. When the excitation voltage is sinusoidal as shown in Fig. 4(a), the flux is also a sinusoidal shape. When the excitation voltage is a two-level square waveform as shown in Fig. 4(b), the flux is a sawtooth shape. The average excitation voltage is adjusted to be zero via the dc-biasing capacitor, and thus, the average flux is also zero. When the excitation voltage is a three-level square voltage as shown in Fig. 4(b), the flux is a trapezoidal shape. The duty cycle is defined as the ratio between the applied high voltage time and the period. In the sawtooth flux, the duty cycle can range from 0% to 100%. In the trapezoidal flux, the duty cycle range from 0% to 50%. At 50% duty cycles, both the sawtooth and trapezoidal waveforms become identical.

It should be noted that only limited ranges of the core loss measurements are executed due to the limitations of the amplifier, such ±75V & ±6A peak ratings and 400V/μs slew rate. The amplifier model number is HSA4014 from NF Corporation. For example, it is difficult to excite the core to high saturation level at high frequency due to limited voltage and current rating of the amplifier. Therefore, the ranges of the experimental results are limited.

Additionally, the core temperature is not closely monitored; however, the core temperature can be assumed to be near room temperature.

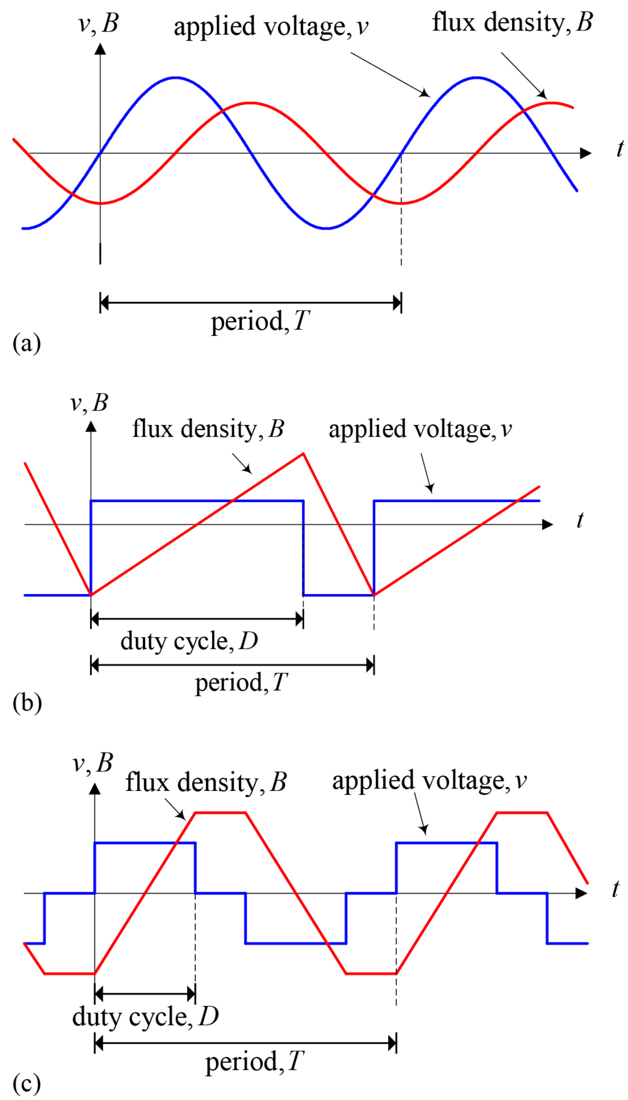

Fig. 4: Excitation voltage waveforms and corresponding flux density waveforms (a) Sinusoidal flux, (b) Sawtooth flux, and (c) Trapezoidal flux

Anhysteritic BH Curves

Fig. 5 illustrates the measured low frequency *BH* loops at 850 Hz. Using the outer most *BH* loop, the anhysteretic *BH* curve is fitted. The anhysteretic *BH* curves can be computed as a function of field intensity *H* using the follow formula.

$$B = \mu_H(H)H$$
$$\mu_H(H) = \mu_0 + \sum_{k=1}^{K} \frac{m_k}{h_k} \frac{1}{1+\left|H/h_k\right|^{n_k}} \tag{3}$$

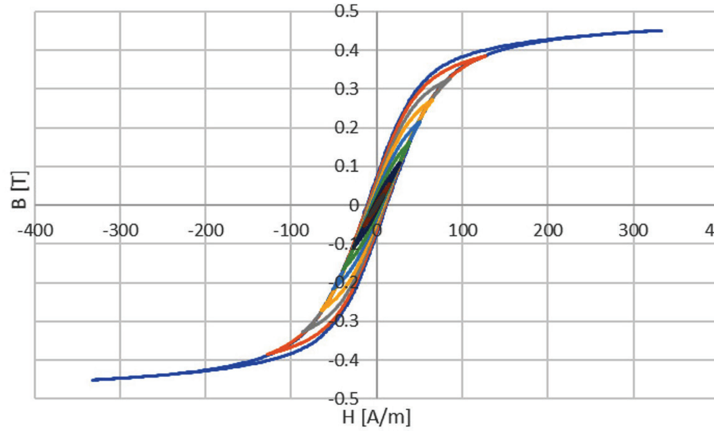

Fig. 5: Low frequency BH loops (excitation at 850 Hz, N_p = 26, N_s = 26)

Similarly, the anhysteretic *BH* curves can be computed as a function of flux density *B* using the follow formula.

$$B = \mu_B(B)H$$
$$\mu_B(B) = \mu_0 \frac{r(B)}{r(B)-1}$$
$$r(B) = \frac{\mu_r}{\mu_r - 1} + \sum_{k=1}^{K} \alpha_k |B| + \delta_k \ln\left(\varepsilon_k + \zeta_k e^{-\beta_k |B|}\right) \tag{4}$$
$$\delta_k = \frac{\alpha_k}{\beta_k}, \varepsilon_k = \frac{e^{-\beta_k \gamma_k}}{1+e^{-\beta_k \gamma_k}}, \zeta_k = \frac{1}{1+e^{-\beta_k \gamma_k}}$$

Table 3 and Table 4 lists the anhysteretic curve coefficients for eqs. (3) and (4), respectively.

The core anhysteretic characteristic models in eqs. (3) and (4) are based on the following references.

Scott D. Sudhoff, "Magnetics and Magnetic Equivalent Circuits," in *Power Magnetic Devices: A Multi-Objective Design Approach*, 1, Wiley-IEEE Press, 2014, pp.488-

G. M. Shane and S. D. Sudhoff, "Refinements in Anhysteretic Characterization and Permeability Modeling," in *IEEE Transactions on Magnetics*, vol. 46, no. 11, pp. 3834-3843, Nov. 2010.

The estimation of the anhysteretic characteristic is performed using a genetic optimization program, which can be found in the following websites:

https://engineering.purdue.edu/ECE/Research/Areas/PEDS/go_system_engineering_toolbox

Table 3: Anhysteretic curve coefficients for B as a function of H

k	1	2	3	4
m_k	0.616043844651630	-0.112194382351634	0.187132470680515	0.320513717783709
h_k	176.000246482166	62.8368237823821	234.277066144063	85.2674214364020
n_k	1	1.14154517453573	2.19358702117813	2.40337698688833

Table 4: Anhysteretic curve coefficients for H as a function of B

k	1	2	3	4
μ_r	4969.05302728848			
α_k	0.776705242579855	0.109358164860025	0.00203334753153070	0.00203305399615861
β_k	91.3631569616114	44.8969014203013	2.33887224273526	16.8800685290068
γ_k	0.551317873846688	0.488944023866976	2.84756007202195	0.351511963614134
δ_k	0.00850129601920617	0.00243576196575954	0.000869370927739407	0.000120441098486359
ε_k	1.33206530923337e-22	2.92641841118830e-10	0.00127940591585760	0.00264207257489038
ζ_k	1	0.999999999707358	0.998720594084142	0.997357927425110

Fig. 6 illustrates the measured *BH* curve and fitted anhysteretic *BH* curves as functions of *H* and *B* using the coefficients from Table 3 and Table 4. Fig. 7 and Fig. 8 illustrates the absolute relative permeability as functions of field strength *H* and flux density *B*, respectively. Fig. 9 illustrates the incremental relative permeability.

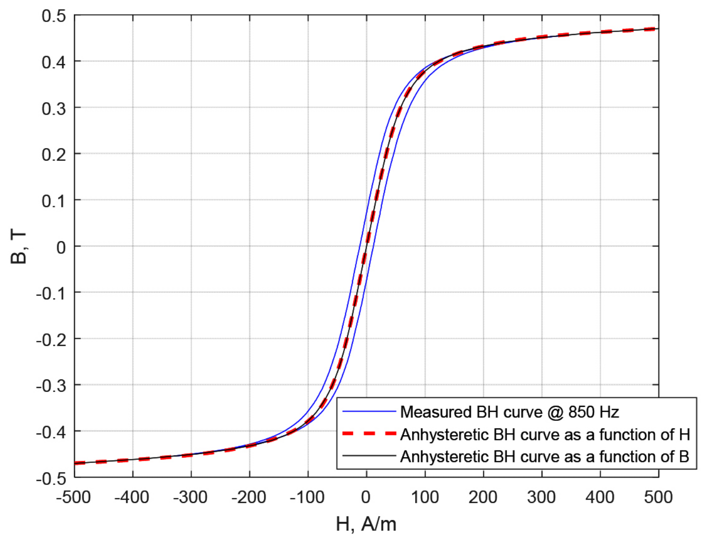

Fig. 6: Measured BH curve and fitted anhysteretic BH curve as functions of H and B

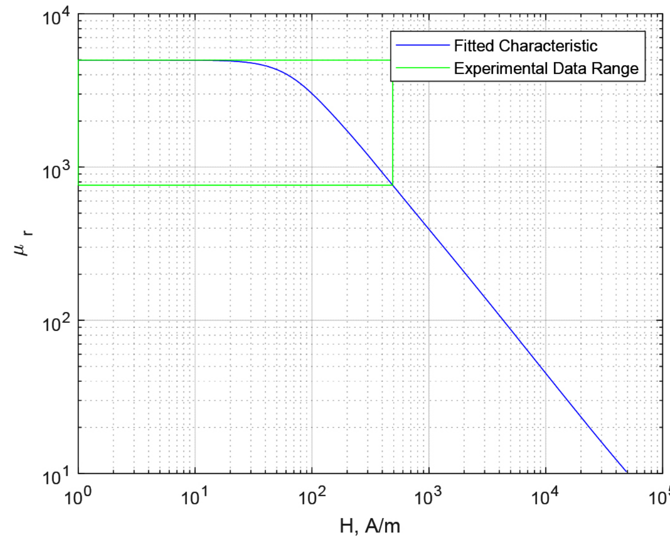

Fig. 7: Absolute relative permeability as function of field strength H

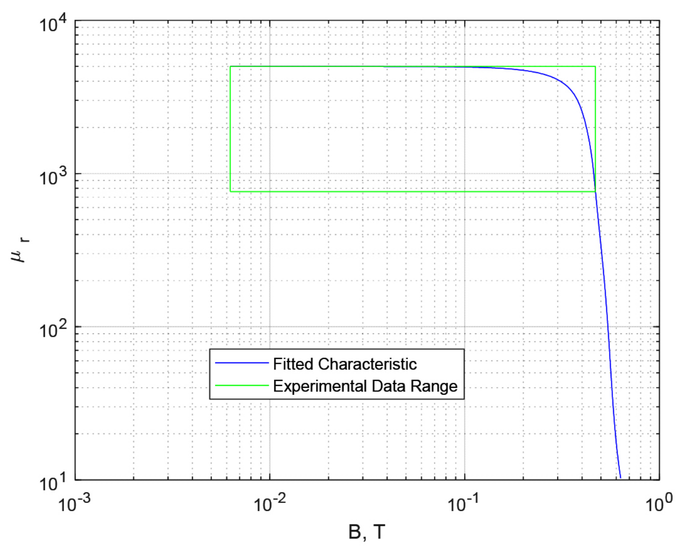

Fig. 8: Absolute relative permeability as function of flux density B

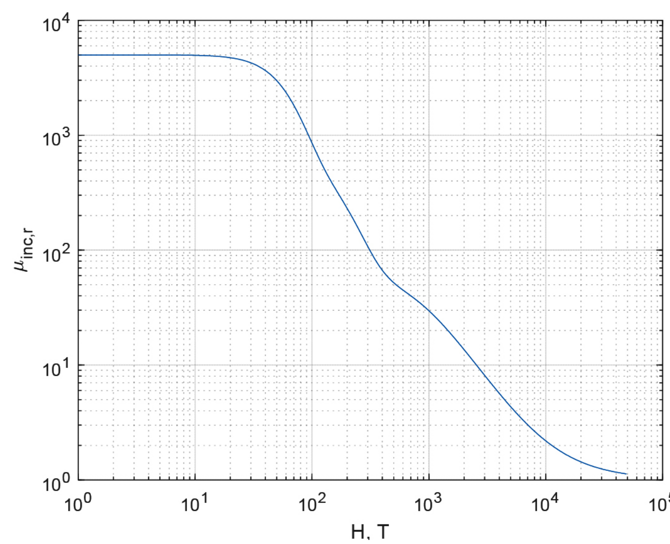

Fig. 9: Incremental relative permeability

Core Losses

Core losses at various frequencies and induction levels are measured using various excitation waveforms. Based on measurements, the coefficients of the Steinmetz's equation are estimated. The Steinmetz's equation is given as

$$P_w = k_w \cdot \left(f / f_0\right)^{\alpha} \cdot \left(B / B_0\right)^{\beta} \tag{5}$$

where P_w is the core loss per unit weight, f_0 is the base frequency, B_0 is the base flux density, and k_w, α, and β are the Steinmetz coefficients from empirical data. In the computation of P_w, the weight in Table 2 is used, the base frequency f_0 is 1 Hz, and the base flux density B_0 is 1 Tesla.

Fig. 10 illustrates the measured *BH* curve at different frequencies. The field strength *H* is kept near constant for all frequency. At 20 kHz and 50 kHz excitations, the *BH* curve is similar, which indicates that the hysteretic losses are the dominant factor at frequencies below 20 Hz. As frequency increases, the *BH* curves become thicker, which indicates that the eddy current and anomalous losses are becoming larger.

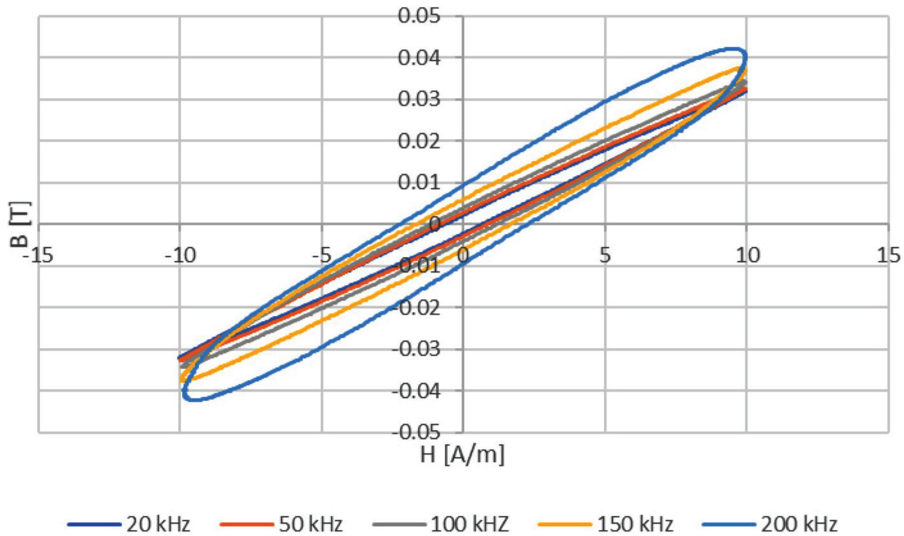

Fig. 10: BH curve as a function of frequency (N_p = 4, N_s = 4, I_p = 9.4A)

Table 5 lists the Steinmetz coefficients at different excitation conditions, and Fig. 11 illustrates the core loss measurements and estimations via Steinmetz equation.

Table 5: Steinmetz coefficients

	k_w	α	β
sine	3.47816153320305e-05	1.63492941721237	2.25271092818147
Sawtooth/Trapezoidal 50% duty	8.13979798102726e-06	1.72243554136948	2.09754521642878
Sawtooth 30% duty	1.13104862883072e-06	1.92376545280231	2.17340478889587
Sawtooth 10% duty	4.97375006995659e-07	1.97641534854932	1.82644558576619
Trapezoidal 30% duty	3.64533125546679e-05	1.65673246622839	2.24624216591967
Trapezoidal 10% duty	5.07821755958067e-07	2.00147824690342	1.84219570683647

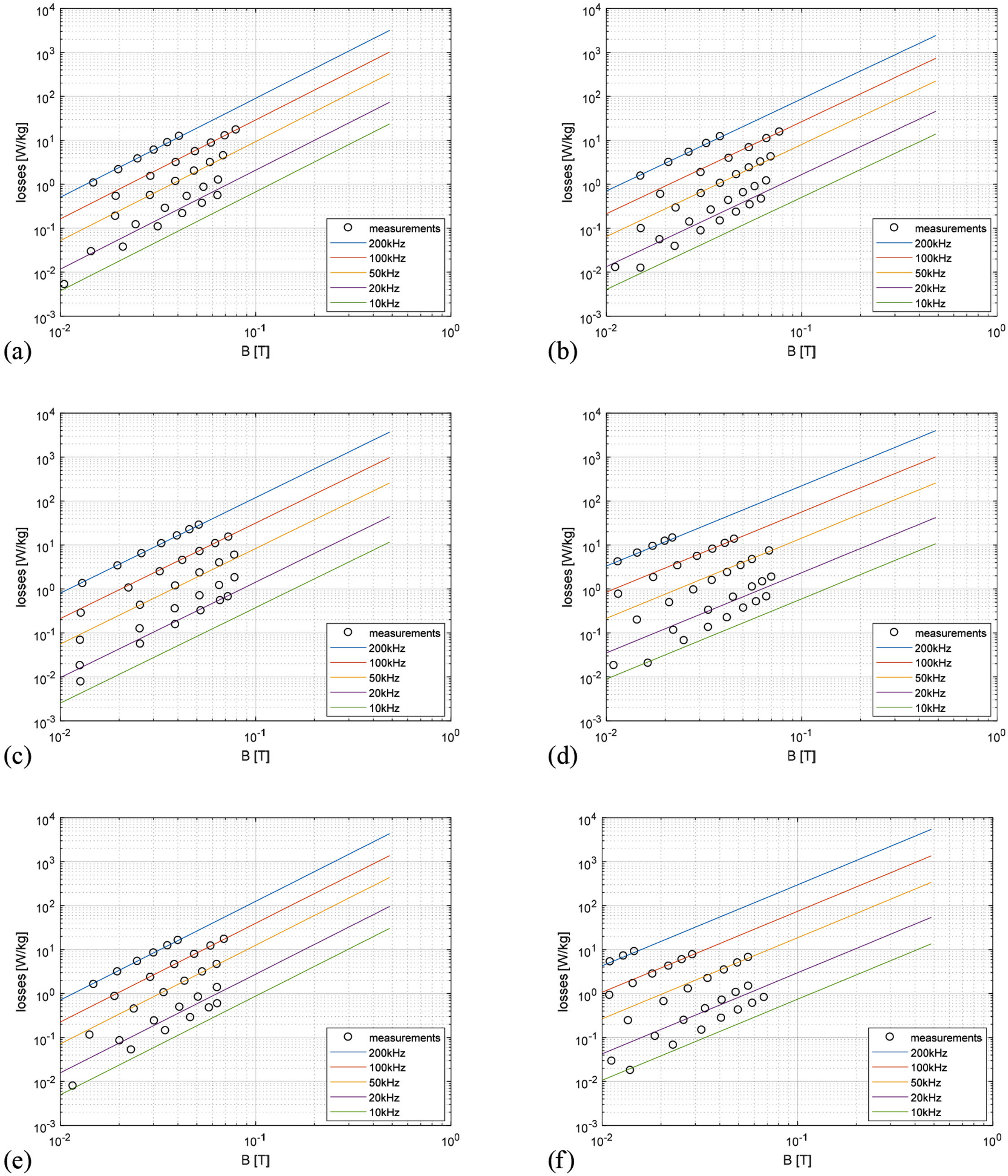

Fig. 11: Core loss measurements and estimations via Steinmetz equation: (a) Sine (b) Sawtooth/Trapezoidal 50% duty (c) Sawtooth 30% duty (d) Sawtooth 10% duty (e) Trapezoidal 30% duty (f) Trapezoidal 10% duty

Core Permeability

The permeability of the core is measured as functions of flux density and frequency. Fig. 12 illustrates the measured absolute relative permeability μ_r values, which is defined as

$$\mu_r = \frac{B_{peak}}{\mu_0 \cdot H_{peak}} \tag{6}$$

where B_{peak} and H_{peak} are the maximum flux density and field strength at each measurement point.

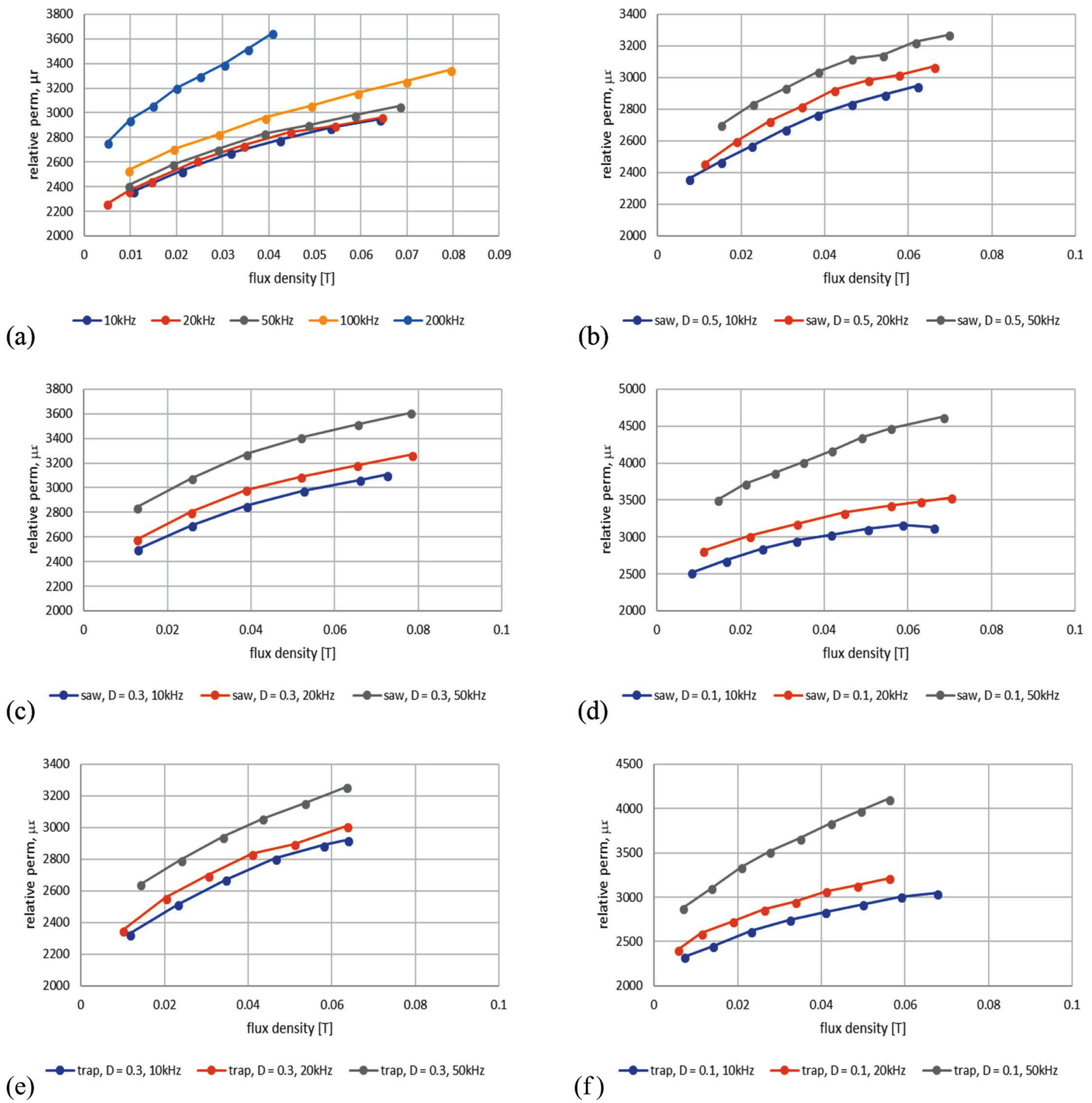

Fig. 12: Relative permeability as a function of flux density and frequency: (a) Sine (b) Sawtooth/Trapezoidal 50% duty (c) Sawtooth 30% duty (d) Sawtooth 10% duty (e) Trapezoidal 30% duty (f) Trapezoidal 10% duty